

The equation of state for non-ideal quark gluon plasma

Abstract

The mass spectra of quarkonium systems at $T = 0$ are analyzed by solving the non-relativistic radial wave equation using the internal energy potential. The QGP matter is studied through the dissociations of quarkonium systems. A modified form of the internal energy potential function is used to determine the EoS at different number of quark flavors by using Mayer's cluster expansion theory and phenomenological thermodynamic model. The thermodynamic model gives a good agreement with the lattice results rather than Mayer's cluster expansion theory. One can conclude that, the Mayer's cluster expansion theory may be more suitable to study a weakly coupled plasma while, the QGP may be considered as a strongly interacting plasma.

keywords: QGP, QCD properties, Mayer cluster expansion

I. Introduction

In the heavy ion collision, there are many signature of deconfinement state creation; one of these signatures is the anomalous suppression of heavy quarkonium production. The heavy mesons produced before the creation formation of a thermalized quark-gluon-plasma and tend to dissociate in the deconfined state. This phenomenon can be described by the screening of the quark-antiquark ($q\bar{q}$) interaction by the large number of color charges in the medium. This mechanism is similar to the Debye screening by electromagnetic charges in the quantum electrodynamics (QED) plasmas [1]. The suppression of heavy quarkonium at finite temperature greater than zero, $T \geq 0$ concerning to the quantum chromodynamics (QCD) has been studied [2]. So that, the dissociation temperature of a particular quarkonium, plays an important role to understand the mechanism of quarkonium dissociation (deconfinement) in the quark-gluon-plasma (QGP). Brambilla et al., [3] have shown that the heavy quark antiquark potential at finite temperature develops an imaginary part that is responsible of the quarkonium dissociation in medium.

The mass spectra at $T = 0$, can be reproduced by using the potential models. So that, the lattice QCD simulations could find a relevant potential term at $T > 0$. This can be done by studying the free energy between a static $q\bar{q}$ pair at finite temperature [4, 5].

37 From the lattice QCD calculations critical temperature; T_c can be determined in which
38 the confining part of the free energy has no effect and vanishes [6].

39 Then the free energy obtained in these calculations can be used to establish the
40 convenient potential model at $T > 0$. However, in other works [7-10], the internal energy
41 can be used as a potential energy. The explanation of how the different potential models
42 be applied to quarkonium states at temperature greater than zero (i.e $T > 0$) is still not
43 completely clarified. Till now, it is believed quantum chromodynamics (QCD) at high
44 temperature to be in a quark gluon plasma (QGP) phase, where color charges may be
45 screened rather than confined [11]. This implies that, at high energy density ε or baryon
46 density ρ , hadron state goes to deconfined state known as the QGP [12].

47 In the recent years, there was a lot of theoretical experimental, and lattice
48 calculation of QCD results. Although there is no confirmed evidence for QGP creation
49 and the order of the phase transition. There is a large amount of study attempts to explain
50 such a matter and the EoS using different models [13-19]. Recently, the Generalized
51 Uncertainty Principle (GUP), used to derive the thermodynamics of ideal Quark-Gluon
52 Plasma (QGP) at a vanishing chemical potential [20].

53 The EoS can be applied directly to study the dynamical quark-gluon plasma (QGP),
54 even in case of interpretation of the heavy-ion experiments or in the framework of the
55 theoretical modeling to study the behavior of hot and dense matter in the early universe
56 [21]. Liu, Shen and Chiang [22] are used the Cornell potential in the approach of
57 Mayer's cluster expansion to calculate the EoS and the energy density of the QGP.

58 In the work we discuss a quantity of interest, the plasma parameter, Γ , which can
59 be defined as the ratio of the potential energy to the kinetic energy. In QED plasma
60 (classical plasma), the parameter has four different regimes: weakly coupled or gas
61 regime for $\Gamma \ll 1$, liquid regime for $\Gamma \approx 1-10$, glassy liquid regime for $\Gamma \approx 10-100$, and
62 solid regime for $\Gamma > 300$ [23]. The plasma parameter Γ is defined as the ratio of
63 potential energy to the kinetic energy $\Gamma = \langle PE \rangle / \langle KE \rangle$.

64 Strongly coupled plasma (SCP) is defined as a plasma in which the plasma
65 parameter is of unit 1 or greater and the Boltzmann distribution for electrons and ions is

66 given by $n_e = n_0 e^{\frac{e\phi}{kT_e}}$ and $n_i = n_0 e^{\frac{-e\phi}{kT_i}}$, respectively [23-28]. This parameter Γ is used
 67 as a measure of the interaction strength in EM plasmas.
 68

69 **II. The Bound State Problem**

70 The bound state energies of heavy quarkonium systems ($c\bar{c}$) and ($b\bar{b}$) are
 71 calculated at different temperatures using the non-relativistic radial wave equation which
 72 given as;

$$73 \quad \left[\frac{d^2}{dr^2} - \frac{l(l+1)}{r^2} - \frac{2\mu}{\hbar^2} V(r, T) + \mathbf{K}^2 \right] \phi_l(r) = 0 \quad (1)$$

74 Where, l is the orbital quantum number, $\mathbf{K}^2 = \frac{2\mu E}{\hbar^2}$ and $\phi_l(r)$ is the radial wave
 75 function. The boundary conditions are given as;

$$76 \quad \phi_l(0) = \phi_l(\infty) = 0 \quad (2)$$

77
 78 $V(r, T)$ can be taken as the internal energy potential $U_1(r, T)$,

$$79 \quad U_1(r, T) = F_1(r, T) - T \cdot \frac{\partial F_1(r, T)}{\partial T} \quad (3)$$

80 Where the free energy potential, $F_1(r, T) = - \frac{4}{3} \frac{\alpha_s}{r} e^{-m_D(T)r}$. And the function
 81 $e^{-m_D(T)r}$ is the screening term [10].

82 In the present work, the free energy function $F_1(r, T)$ can be modified through
 83 adding a linear term; due to the confinement behavior of the strong interactions at large
 84 distances;

$$85 \quad F_1(r, T) = - \left(\frac{4}{3} \frac{\alpha_s(T)}{r} - C r \right) e^{-m_D(T)r} \quad (4)$$

86 Where, C is a free parameter, and $\alpha_s(T)$ is the running coupling constant which is given
 87 by;

$$88 \quad \alpha_s(T) = \frac{2\pi}{(11 - \frac{2}{3}n_f) \ln(\frac{T}{\Lambda_\sigma})} \quad (5)$$

Where, n_f is the number of quark flavors, ($n_f = 0, 2, 3$). From lattice QCD computations [10], the parameter $\Lambda_\sigma = \beta T_c$ where, $\beta = 0.104 \pm 0.009$.

In the present work, T_c is taken as, $T_c = 0.2$ GeV. The Debye screening mass $m_D(T)$ [29] is given by [10],

$$m_D(T) = \gamma \cdot \alpha_s(T) \cdot T, \quad (6)$$

Where, $\gamma = 4\pi\eta c_\sigma$. In table (1) all the parameters used are listed.

Table (1) The parameters of the internal energy

Parameter	Value	Ref.
β	0.104 ± 0.009	[4,10]
c_σ	0.566 ± 0.013	[4, 10]
η	2.06	[4, 10]
T_c	0.2 GeV	Present work
C	$0.135 \pm 0.015 \text{ GeV}^2$	Present work
m_c	$1.361 \pm 0.022 \text{ GeV}$	Present work
m_b	$4.694 \pm 0.063 \text{ GeV}$	Present work

According to eqs. (3, 4), the internal energy potential can be rewritten as,

$$U_1(r, T) = -\left(\frac{4}{3} \frac{\alpha_s(T)}{r} - Cr\right) e^{-m_D(T)r} - \frac{4}{3} T \left[\gamma \cdot \frac{A_1}{A_2} \left(\alpha_s(T) - \frac{A_1}{A_2^2} \right) + \frac{A_1}{T A_2^2} \cdot \frac{1}{r} \right] e^{-m_D(T)r} \\ + C \cdot T \cdot r^2 \cdot \gamma \left(\alpha_s(T) - \frac{A_1}{A_2^2} \right) e^{-m_D(T)r} \quad (7)$$

For simplicity, $A_1 = \frac{2\pi}{(11 - \frac{2}{3}n_f)}$ and $A_2 = \ell n\left(\frac{T}{\Lambda_\sigma}\right)$

The total mass of the different quarkonium states (resonance masses) is given by;

$$M_{nl} = 2m_q + \varepsilon_{nl} \quad (8)$$

Where, m_q is the quark mass, and ε_{nl} is the “binding energy”. Equation (1) can be re-written as,

$$\frac{d^2 \phi_l(r)}{dr^2} + [\lambda - C(r, T)] \phi_l(r) = 0 \quad (9)$$

$$\text{Where, } \hbar = 1, \lambda \equiv K^2 = \frac{2\mu E}{\hbar^2} \quad \text{and} \quad C(r, T) = 2\mu V(r, T) + \frac{l(l+1)}{r^2}$$

Introducing the dimensionless variables t and $\rho_l(t)$ [30, 31] in equation (9) where,

$$t = \frac{1}{1 + \frac{r}{r_0}} \quad \text{and} \quad \rho_l(t) = t \phi_l(r) \quad \text{Where, } r_0 = 1 \text{ GeV}^{-1} \quad \text{one gets,}$$

$$\frac{d^2 \rho_l}{dt^2} + \frac{r_0^2}{t^4} [\lambda - C(t, T)] \rho_l(t) = 0 \quad (10)$$

121

122 With the boundary conditions,

$$\rho_l(0) = 1, \quad \rho_l(1) = 0 \quad (11)$$

124 To transform eq. (10) to a true eigen-value equation, the range of t from (0, 1) can be
125 divided into $(n+2)$ points with the interval h and labeled with subscript j and the
126 boundary conditions (11) at $j = 0$ and $n+1$ can be written as,

$$\rho_0 = \rho_{n+1} = 1 \quad (12)$$

128 Using the finite difference approximation [32],

$$\frac{d^2 \rho}{dt^2} = \frac{1}{12h^2} (-\rho_{j-2} + 16\rho_{j-1} - 30\rho_j + 16\rho_{j+1} - \rho_{j+2}) + O(h^4) \quad (13)$$

130 Substitute into eq. (10) one gets,

$$(-\rho_{j-2} + 16\rho_{j-1} - 30\rho_j + 16\rho_{j+1} - \rho_{j+2}) + \frac{12h^2}{(jh)^4} [C(jh, T) - \lambda] \rho_j = 0 \quad (14)$$

132 Equation (14) is a set of linear equations in ρ_j and can be written in the matrix form,

$$S \rho = 0 \quad (15)$$

Where S is a $(n \times n)$ symmetric matrix and ρ is n -dimensional column matrix. Eq. (15) can be transformed to a true eigen-value equation and solved numerically by using Jacobi method [32, 33].

Table (2) is a list of the resonance masses M_{nl} in (GeV) of $c\bar{c}$ and $b\bar{b}$ states. We have calculated them by solving the Schrödinger equation numerically by using the internal energy potential at $T = 0$. In table (2) the calculated masses of $c\bar{c}$ and $b\bar{b}$ states according to different previous potential forms and the internal energy potential are given. One can see that the masses calculated by using the internal energy potential are very close to the experimental data.

Table (2): The mass spectra of $c\bar{c}$ and $b\bar{b}$ bound states by using the internal energy potential compared to the experimental masses and other theoretical potentials.

	nl	State (GeV) M_{nl} [22, 34,35]	The present work	Cornell potential [22]	Phenomenological potential [34]
$c\bar{c}$	1S	J/ψ (3.097 ± 0.001)	3.097	3.0697	3.097
	2S	ψ' (3.686 ± 0.0027)	3.687	3.6978	3.684
	3S	ψ'' (4.040 ± 0.0027)	4.047	4.1696	4.096
	4S	ψ (4.415 ± 0.0062)	4.415	-	4.427
	1P	χ_c (3.506 ± 0.0041)	3.500	3.5003	3.520
	1D	ψ (3.768 ± 0.0036)	3.769	-	3.671
	2D	ψ (4.159 ± 0.02)	4.134	-	4.076
$b\bar{b}$	nl	State (GeV) M_{nl} [22, 34,35]	The present work	Cornell potential [22]	Screened potential [35]
	1S	Y (9.460 ± 0.00026)	9.460	9.4450	9.460
	2S	Y' (10.0233 ± 0.00031)	10.0227	10.0040	10.016
	3S	Y'' (10.3553 ± 0.0005)	10.3551	10.3547	10.351
	4S	Y (10.580 ± 1.0002)	10.580	-	10.611
	5S	$Y(10.865 \pm 0.0008)$	10.7808	-	10.831
	1P	χ_b (9.9002 ± 0.00026)	9.9003	9.8974	9.918
	2P	χ_b (10.268 ± 0.00022)	10.2522	-	10.269
	1D	ψ (10.161 ± 0.0006)	10.1557	-	10.156

III. The QGP equation of state by using Mayer's cluster expansion theory

Mayer's theory of plasma is described in [36, 37]. The EoS is one of the most basic information in the case of studying the QGP matter;

$$\frac{P}{T} = n_q + n_{\bar{q}} + S - n_q \frac{\partial S}{\partial n_q} - n_{\bar{q}} \frac{\partial S}{\partial n_{\bar{q}}} \quad (16)$$

Where P, T, n_q , $n_{\bar{q}}$ are the pressure, the temperature, the densities of the quarks and the antiquarks, respectively. The entropy S is given by [36],

$$S = \int dI \sum_{\nu \geq 1} \frac{1}{16\pi^3} (-k^2)^\nu V_\ell^{\nu+1}, \quad (17)$$

Where, $k^2 = \frac{n_q + n_{\bar{q}}}{T}$, V_ℓ is the interaction potential in the momentum space and

$dI = 4\pi \ell^2 d\ell$, therefore,

$$\frac{\partial S}{\partial k^2} = \frac{k^2}{4\pi^2} \int_0^\infty d\ell \frac{V_\ell^2}{1 + k^2 V_\ell} \quad (18)$$

Therefore equation (16) can be written as;

$$\frac{P}{T} = k^2 T + S - k^2 \frac{\partial S}{\partial k^2} \quad (19)$$

So, the internal energy potential eq. (7) can be transformed by Fourier transformation to the momentum space and rewritten as,

$$\begin{aligned} U_1(\ell, T) = & \frac{-16\pi}{3} \frac{\alpha_s(T)}{\ell^2 + m_D^2(T)} + \frac{16\pi C m_D(T)}{(\ell^2 + m_D^2(T))^2} \\ & - \frac{32}{3} \pi T \gamma \alpha_s(T) \cdot m_D(T) \left(\frac{-A_1 + A_1 \cdot A_2}{A_2^2} \right) \frac{1}{m_D^2 + \ell^2} \\ & - \frac{16\pi}{\ell^2 + m_D^2(T)} \left(\frac{A_1}{A_2^2} \right) + 96 \pi C T \gamma m_D(T) \cdot \left(\frac{-A_1 + A_1 \cdot A_2}{A_2^2} \right) \cdot \left(\frac{m_D^2(T) - \ell^2}{(\ell^2 + m_D^2(T))^2} \right) \end{aligned}$$

167

168

169

170

(20)

171 The energy density can be calculated by the following relation [10]

$$\varepsilon = T \frac{\partial P}{\partial T} - P \quad (21)$$

173 Taking $k^2 \approx a_f T^2$ in which, a_f is the Stefan-Boltzmann constant [38] is given by,

$$a_f = (16 + \frac{21}{2} n_f) \frac{\pi^2}{90} \quad (22)$$

175

176 **IV. The phenomenological thermodynamic model**177 The EoS of SCP as a function of Γ is given as [24] ,

$$\varepsilon_{QED} = \left(\frac{3}{2} + U_{ex}(\Gamma) \right) nT \quad (23)$$

179 Where, $U_{ex}(\Gamma)$ is the non-ideal or excess contribution to EoS and is given as [24];

$$U_{ex}(\Gamma) = \frac{U_{ex}^{Abe}(\Gamma) + 3 \times 10^3 \Gamma^{5.7} U_{ex}^{OCP}(\Gamma)}{1 + 3 \times 10^3 \Gamma^{5.7}} \quad (24)$$

181 Where the functions of $U_{ex}^{Abe}(\Gamma)$, $U_{ex}^{OCP}(\Gamma)$ are given as [24];

$$U_{ex}^{Abe}(\Gamma) = \frac{-\sqrt{2}}{2} \Gamma^{3/2} - 3\Gamma^3 \left[\frac{3}{8} \ln(3\Gamma) + \frac{\gamma}{2} - \frac{1}{3} \right] \quad (25)$$

183

$$U_{ex}^{OCP}(\Gamma) = -0.898004 \Gamma + 0.96786 \Gamma^{1/4} + 0.220703 \Gamma^{-1/4} - 0.86097 \quad (26)$$

185

186 The term U_{ex}^{Abe} was derived by Abe [39] and is valid for $\Gamma < 0.1$, and $\gamma = 0.57721...$ is187 the Euler's constant. The term U_{ex}^{OCP} determined by simulation of one component

188 plasma (OCP). The OCP is occurred when a single species of charged particles

189 distributed in a uniform background of neutral charges, and is valid for $1 \leq \Gamma < 180$.

190 Considering the model proposed by Bannur [24] that the hadron (confined state) exists at
 191 $T < T_c$ and goes to QGP (deconfined state) at $T > T_c$. In ref. [24] the plasma parameter Γ
 192 is determined for the Coulomb potential.

$$193 \quad \Gamma \equiv \frac{\langle PE \rangle}{\langle KE \rangle} = \frac{4\alpha_s}{3r_{av} T} \quad (27)$$

194 The coupling constant $\alpha_s \approx 0.5$, $r_{av} \approx 1\text{fm}$, $r_{av} = \left(\frac{3}{4\pi n}\right)^{1/3}$, where “n” is the density.

195 In the present work the plasma parameter Γ is calculated quantum mechanically as,

$$196 \quad \langle Q \rangle = \int \psi^* \hat{Q} \psi d\tau$$

197 In which we have used the wave function (eigen-function) that produced for the
 198 calculation of the bound state energies (eigen-values). For the SCQGP model of eq. (23)
 199 to include the relativistic quantum effects as indicated in ref. [24]. Hence, eq. (23) can be
 200 re-written as,

$$201 \quad \varepsilon = (2.7 + U_{ex}(\Gamma)) n T \quad (28)$$

202 Where the first term ($2.7 n T$) corresponds to the ideal EoS, which may be written as,

$$203 \quad \varepsilon_s = 3 a_f T^4 .$$

$$204 \quad \frac{\varepsilon_s}{n} = \frac{3a_f T^4}{1.1a_f T^3} = 2.7 T \quad (29)$$

205 One can calculate the expectation value of the internal energy potential from the wave
 206 function reproduced from solving of the Schrödinger. From eq. (29) one obtains $e(\Gamma)$ the
 207 energy density normalized to the ideal one:

$$208 \quad e(\Gamma) \equiv \frac{\varepsilon}{\varepsilon_s} = 1 + \frac{1}{2.7} U_{ex}(\Gamma) \quad (30)$$

209 From eq.(21) and eq. (28) one can get the EoS (pressure) as following,

$$210 \quad \frac{P}{T^4} = \left(\frac{P_0}{T_0} + 3a_f \int_{T_0}^T d\tau \tau^2 e(\Gamma) \right) \quad (31)$$

211 Where P_0 , is the pressure at temperature T_0 and may be taken from one of the lattice data
 212 points or at critical temperature T_c .

V. Results and discussion

In figure (1) the internal energy potential $U_1(r, T)$ eq. (7) versus r is plotted at $T = 0$ and compared with the Cornell potential [22]. Also, it is plotted at different temperature values, $T = (0.5-1.5)T_c$. One can notice that, at small r both potentials behave similarly approximately and intersect at $r \approx 1 \text{ GeV}^{-1}$ in which the Coulomb term is more effective. At large distances the behavior of both potential forms is completely different where the confinement term of the potential is more effective. Also, the behavior of the deconfinement mechanism at large separation (r) and high temperature ($T > T_c$) is shown.

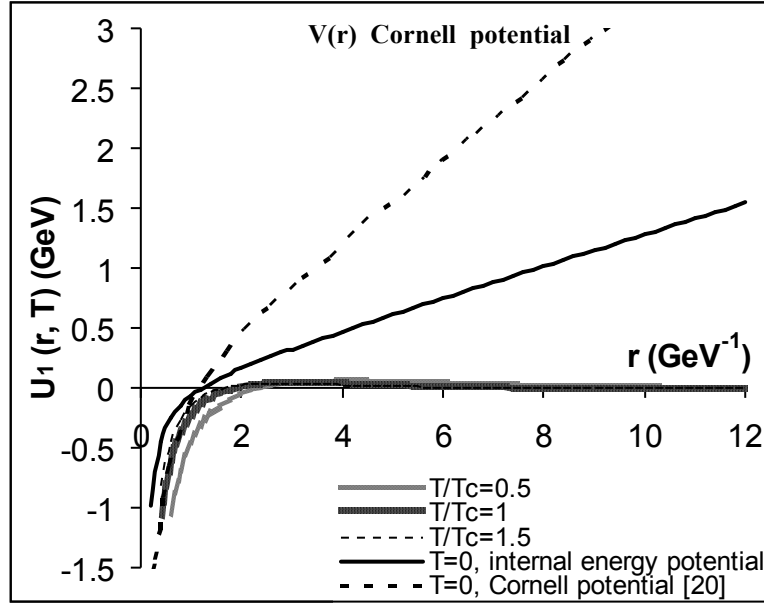


Fig. (1) The internal energy potential $U_1(r, T)$ versus r at different temperature $T = (0.5-1.5)T_c$ and at $T = 0$.

In figure (2) the running coupling constant $\alpha_s(T)$ versus temperature T is plotted at different number of quark flavors. One can see that, the running coupling decreases logarithmically as T increases for different number of flavors ($n_f = 0, 2, 3$). The behavior of the Debye screening mass at different temperature is studied [see figure (3)]. This figure

shows the calculated values of the Debye screening mass; m_D ; versus T/T_c and the lattice results [10, 29]. In this case the results predict that; $m_D(T) \propto \alpha_s(T) \cdot T$, instead of the usual dependence $\sqrt{\alpha_s(T)} T$ [10].

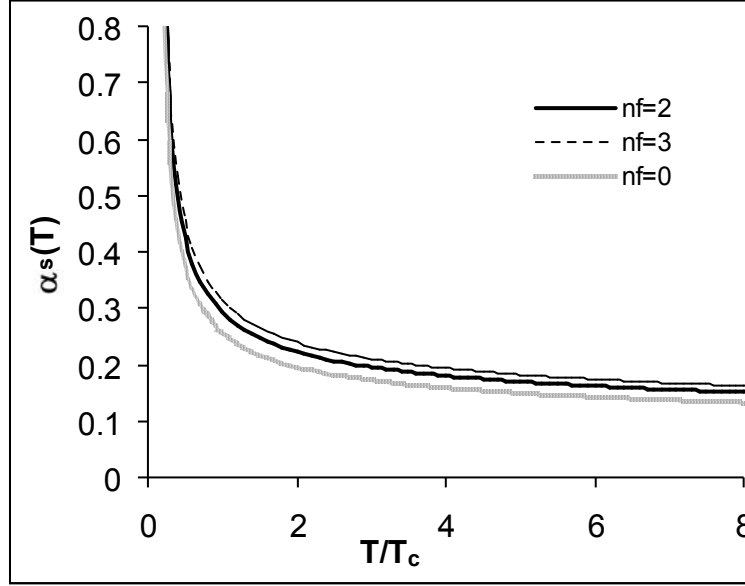


Fig. (2) The running coupling constant $\alpha_s(T)$ versus T/T_c at different number of quark flavors $n_f = 0, 2, 3$.

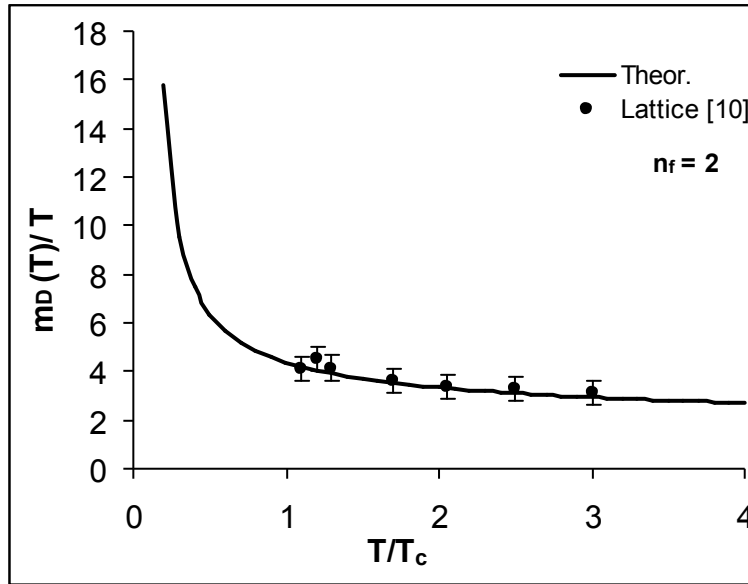


Fig. (3) The Debye screening mass $m_D(T)/T$ versus T/T_c compared with the lattice data [10].

Figure (4) shows the theoretical calculation of the EoS using Mayer's expansion theory; from eq. (19) at different number of quark flavors $n_f = 0, 2, 3$.

In the present calculations the critical temperature is taken as, $T_c = 0.2$ GeV. The solid line and the different dashed lines represent the theoretical calculations by using Mayer's cluster expansion theory and the symbols are the lattice results. It is clear that, a suitable qualitative agreement between the theoretical calculation and the lattice results especially at the intermediate temperature range at $n_f = 0$. While at $n_f = 2$, it is clear that the present theoretical calculation does not match the lattice results. However, at $n_f = 3$ a qualitative agreement between the present calculations and the lattice results are obtained.

Generally one can conclude that, the Mayer's cluster expansion theory is more suitable to study a weakly coupled plasma, while the QGP may be strongly coupled plasma [14].

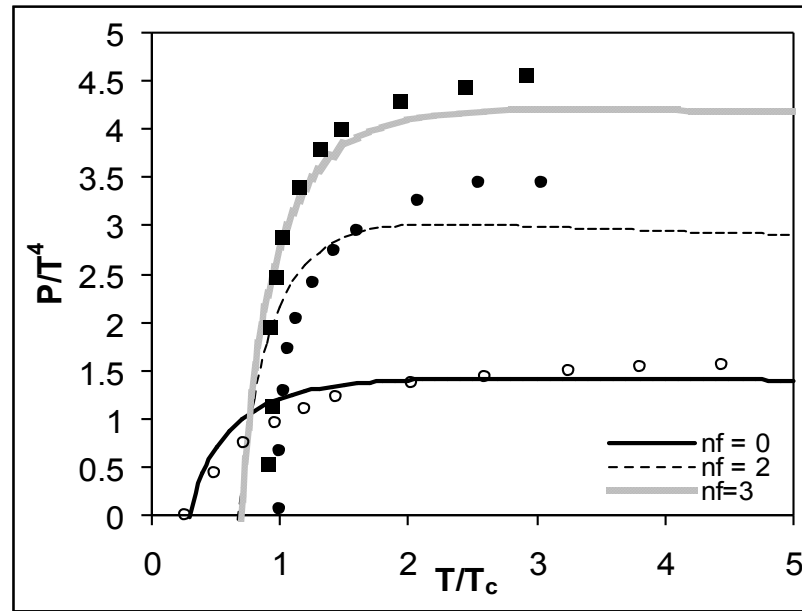


Fig. (4) The equation of state P/T^4 versus T/T_c , $T_c = 200$ MeV, (solid and dashed lines) are the theoretical calculations and (symbols) are the lattice results [24, 40].

Figure (5) shows the calculated energy density \mathcal{E}/T^4 by using Mayer's cluster expansion theory at different number of quark flavors, $n_f = 0, 2, 3$ versus T/T_c . The solid and dashed lines are the theoretical calculations and the symbols are the lattice results. From this fig. one can see that, at $n_f=0$, a qualitative agreement between the present calculations and the lattice results is obtained at high temperatures, but at $T < 2T_c$ the theoretical calculation does not match the lattice results. While at $n_f=2$ it is clear that, the theoretical calculations doesnot give agreement with the lattice results at small temperature range. But at $n_f=3$ it is clear that, the theoretical calculation matches with the lattice results especially at high temperature range.

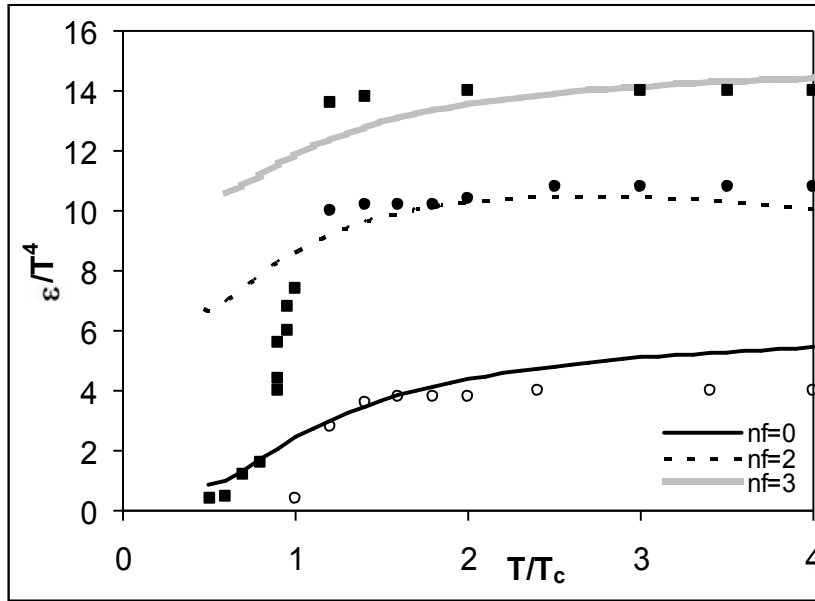


Fig. (5) The equation of state \mathcal{E}/T^4 versus T/T_c , $T_c = 200$ MeV, (solid & dashed lines) are the theoretical calculations and (symbols) are the lattice results [22, 40].

In the present work the plasma parameter is calculated quantum mechanically using the wave function produced from the numerical solution of the Schrödinger equation for quarkonium bound state system. Figure (6) shows the behavior of the calculated plasma parameter $\Gamma(T)$ using the internal energy potential. It is clear that, the largest value at $T/T_c \approx 1$, and tends to zero at very high temperature $T/T_c \approx 5$.

Equations (31) are used to calculate the EoS by using a phenomenological thermodynamic model. Figure (7) shows the present calculations of the equation of state (EoS) versus T/T_c at different number of quark flavors ($n_f = 0, 2, 3$) in comparison with the theoretical calculations of the Cornell potential [24] and the lattice results .

From this figure, one can see that, the present calculations of the EoS using the internal energy potential give more agreement with the lattice results than the Cornell potential calculations at $n_f = 0, 3$. But at $n_f = 2$ it is clear that, the Cornell potential calculations give more agreement in this case with the lattice results.

The behavior of the energy density ε/T^4 versus T/T_c is calculated by using equation (30), at different number of quark flavors, $n_f = (0, 2, 3)$.

In figure (8), the solid lines represent the present calculations of the EoS by using the internal energy potential, the dashed lines are the theoretical calculations by using Cornell potential [24], and the symbols are the lattice results [24, 41, 42].

From figure (8) one can see that, the present calculations using the modified internal energy potential give a satisfied agreement at all temperature range with the lattice results compared with the Cornell potential calculations, especially at $n_f = 0, 3$. While at $n_f = 2$ the Cornell potential calculations give a slight better fit with the lattice results.

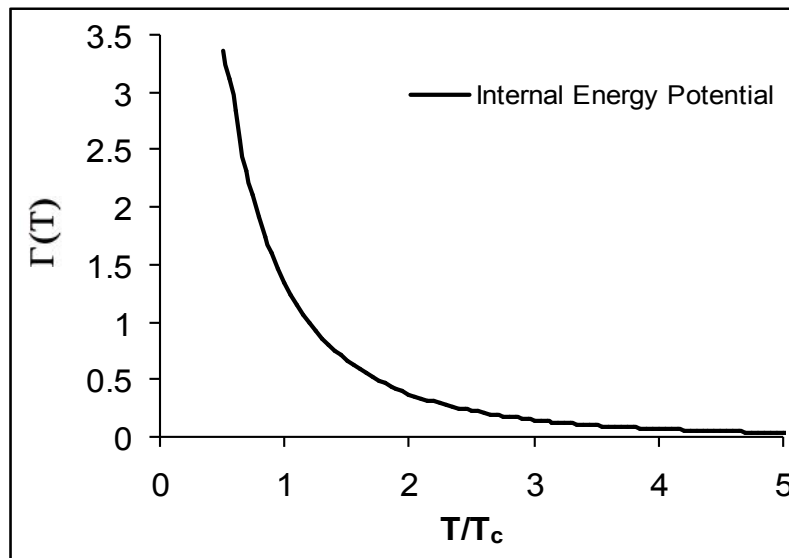


Fig. (6) The plasma parameter $\Gamma(T)$ versus T/T_c calculated by the internal energy potential.

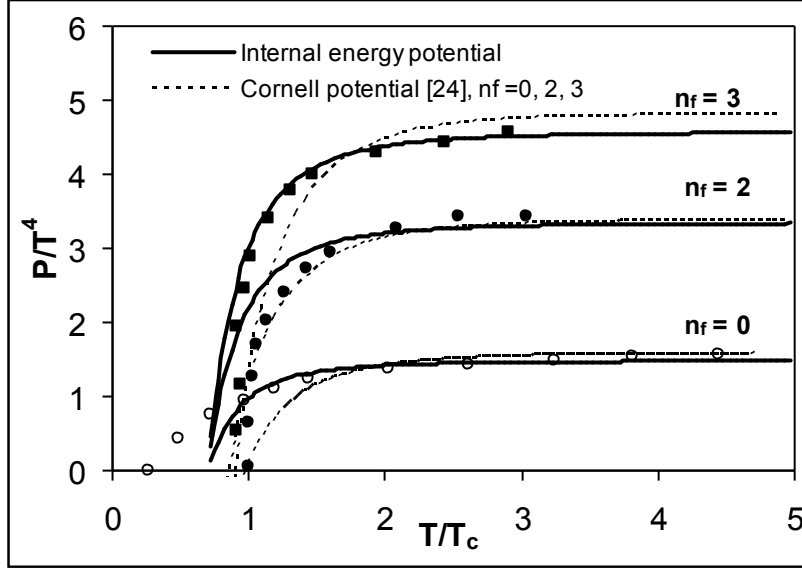


Fig. (7) The equation of state P/T^4 versus T/T_c , $T_c = 200$ MeV, (solid lines) are the theoretical calculations, dashed lines are the EoS calculated by Cornell potential and (symbols) are the lattice results [24,40].

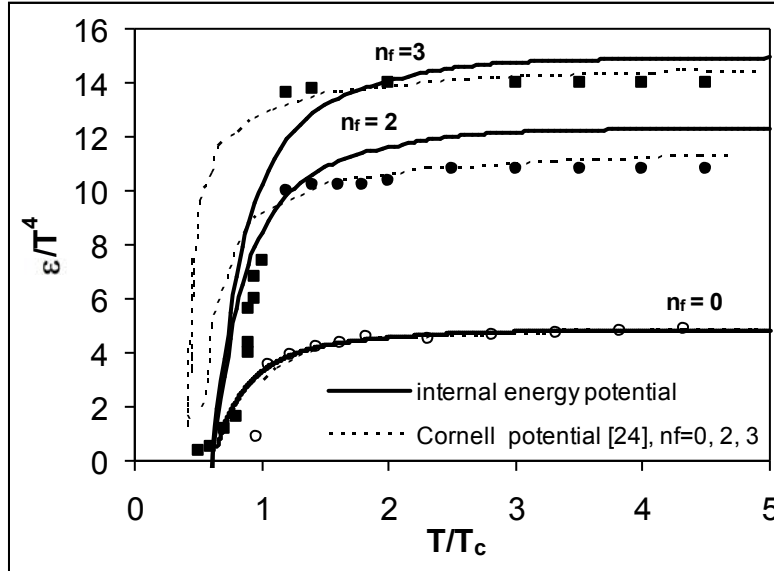


Fig. (8) The energy density ε/T^4 versus T/T_c , $T_c = 200$ MeV, (solid lines) are the theoretical calculations, dashed lines are the EoS calculated by Cornell potential and (symbols) are the lattice results [24,40].

Once the pressure (P) and the energy density (ε) are calculated, one can calculate the trace anomaly or the interaction measure quantity (Δ), which is one of the most important quantities in the studying of the quark-gluon plasma phase transition.

In figure (9) the interaction measure; $\Delta = \frac{\varepsilon - 3P}{T^4}$; is plotted versus T/T_c with the lattice results [24, 41]. In this figure we have calculated the deviation between the energy density ε of the QGP system and the corresponding one in case of the ideal gas plasma ($P = \frac{1}{3}\varepsilon$). From this figure one can see that, Δ tends to zero for large T and Δ still has value and does not vanish up to $T \approx 3T_c$ [2, 42].

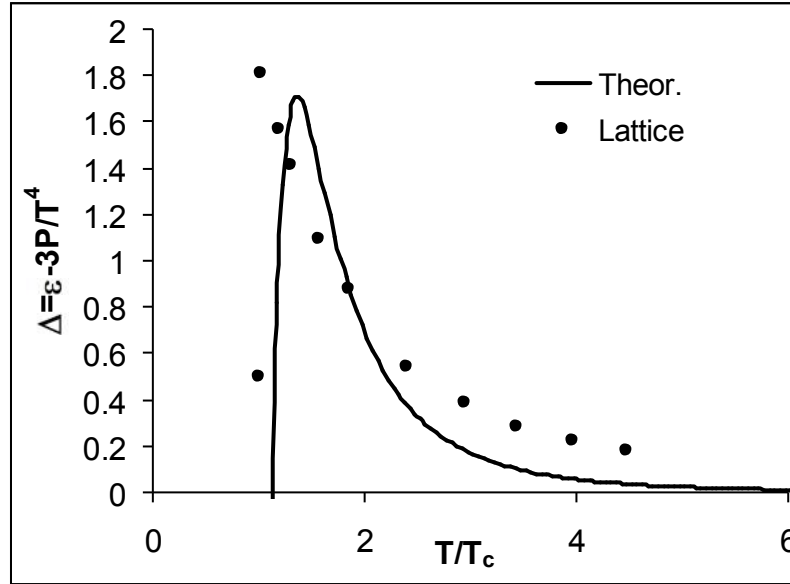


Fig. (9) The deviation $\Delta = \frac{\varepsilon - 3P}{T^4}$ versus T/T_c , the solid line is the theoretical calculations and the symbols are the lattice results [41].

Conclusion

In this work, we introduce a linear term to the internal energy potential function. This modification provided a linear part within the effect of the screening term in both parts of the free energy function. Then we have studied the applicability of using this potential form to the dissociations of $c\bar{c}$ and $b\bar{b}$ systems, and the study of the equation of state for such matter. From these calculations, the Mayer's cluster expansion theory has shown poor fit with the lattice results. So that, Mayer's cluster expansion may be more suitable to study a weakly coupled plasma while the QGP may be considered as a strongly interacting plasma.

The thermodynamic model calculations depending on the plasma parameter $\Gamma(T)$ have shown a reasonable fit at low and high temperatures with the lattice results. Therefore, this phenomenological model is more applicable to describe the EoS of the QGP matter rather than the Mayer's cluster expansion theory.

References

- [1] T. Matsui and H. Satz, Phys. Lett. B 178,, 416 (1986).
- [2] H. Satz, J. Phys. G 32, R25(2006), hep-ph/0512217.
- [3] Nora Brambilla, Jacopo Ghiglieri, Peter Petreczky, Antonio Vairo, Phys. Rev. D 78, 014017 (2008), hep-ph/0804.0993.
- [4] G. Boyd et al., Nucl. Phys. B 469, 419 (1996), hep-lat/9602007.
- [5] Y. Maezawa et al., Phys. Rev. D 75, 074501 (2007), hep-lat/0702004.
- [6] F. Karsch, E. Laermann, and A. Peikert, Nucl. Phys. B 605, 579 (2001), hep-lat/0012023.
- [7] W.M. Alberico, A. Beraudo, A. De Pace and A. Molinari Phys. Rev. D 72, 114011 (2005), hep-ph/0507084v1.
- [8] E. V. Shuryak and I. Zahed, Phys. Rev. D 70, 054507 (2004), hep-ph/0403127.
- [9] W. M. Alberico, A. Beraudo, A. De Pace, and A. Molinari, Phys. Rev. D 75, 074009 (2007), hep-ph/0609116.
- [10] F. Brau, and F. Buisseret, Phys. Rev. C 76, 065212 (2007).

445 [11] Boris A. Gelman^{1, 2}, Edward V. Shuryak¹ and Ismail Zahed, Phys. Rev. C74,
 446 044909 (2006), nucl-th/0605046v1.
 447 [12] J. Cleymans, R. V. Gavai and E. Suhonen, Phys. Rep. 130, 217 (1986).
 448 [13] V. M. Bannur, Phys. Lett. B 362, 7 (1995).
 449 [14] K. M. Udayanandan, P. Sethumadhavan, and V. M. Bannur, Phys. Rev. C 76,
 450 044908 (2007).
 451 [15] M. Bluhm B. Kampfer, R. Schulze, D. Seipt , Contribution to the International
 452 School of Nuclear Physics - 30th Course: Heavy-Ion Collisions from the Coulomb
 453 Barrier to the Quark-Gluon Plasma, Erice, Sicily, Italy, 16-24 Sep (2008), hep-
 454 ph/0901.0472v1.
 455 [16] L.M. Satarov, M.N. Dmitriev, I.N. Mishustin, Phys. Atom. Nucl.72, 1390 (2009),
 456 hep-ph/0901.1430v1.
 457 [17] Raghunath Sahoo, Tapan K. Nayak, Jan-e Alam, Sonia Kabana, Basanta K. Nandi, D. P.
 458 Mahapatra, Presented in SQM08, J. Phys. G36, 064071 (2009), nucl-ex/0901.3254v1.
 459 [18] E.V.Komarov, Yu.A.Simonov, talk given at "13th Lomonosov Conference on
 460 Elementary Particle Physics", Moscow, August 23 - 29, (2007), hep-ph/0801.2251v2.
 461 [19] Ariel R. Zhitnitsky, Nuclear Physics A 813, 279 (2008).
 462 [20] N.M. El Naggat, L. I. Abou-Salem, I. A. Elmashad, A.F. Ali, J. Mod. Phys.4, No. 4A,,
 463 13 (2013).
 464 [21] Michael Cheng, Proceedings of the XXV International Symposium on Lattice Field
 465 Theory, Regensburg, Germany (2007), hep-lat/0710.4357v1.
 466 [22] B. Liu, P. N. Shen and H. C. Chiang, Phys. Rev. C55, No.6, 3021 (1997).
 467 [23] Edward Shuryak, Prog.Part.Nucl.Phys.62, 48(2009), hep- ph/ 0807.3033v2.
 468 [24] V.M. Bannur, J. Phys. G32, 993 (2006), hep-ph/0504072v2.
 469 [25] S. Ichimaru, Statistical Plasma Physics (Vol. II) - Condensed Plasma (Addison-
 470 Wesley Publishing Company, New York), (1994).
 471 [26] V. M. Bannur, hep-ph /0807.2092v1.
 472 [27] R. Rapp, D. Cabrera, V. Greco, M. Mannarelli and H. van Hees, Winter Workshop
 473 on Nuclear Dynamics, South Padre Island (TX, USA), April 05-12 (2008), hep-
 474 ph/0806.3341v1.
 475 [28] J. L. Nagle, Eur. Phys. J. C49, 275 (2007) , nucl-th/0608070 v1.

- [29] N. O. Agasian and Yu. A. Simonov, Phys. Lett. B 639, 82 (2006), hep-ph/0604004.
- [30] L. I. Abou-Salem, Int. J. Mod. Phys. A20, 4113 (2005), L. I. Abou-Salem, J. Phys. G: Nuclear and Particle Physics 30, 1391(2004).
- [31] A. G. Tsypkin and G. G. Tsypkin, mathematical formulas, Mir publisher, Moscow (1988).
- [32] S. M. Wong, computational methods in physics and engineering, © by Prentice – Hall, Inc. (1992).
- [33] A. R. Gourlay, and G. A. Watson, computational methods for matrix eigenproblems, © John Wiley & Sons Ltd (1973).
- [34] Jinfeng Liao and Edward Shuryak, Phys. Rev. C75, 054907 (2007).
- [35] O. Portilho and Z.M.O. Shokranian, Revista Brasileira de Física, Vol.14, No. 1, (1984).
- [36] R. Balescu, Statistical Mechanics of Charged Particles © Interscience Publishers, London (1963).
- [37] D. Kremp, M. Schlanges and W. D. Kraeft, Quantum Statistics of Nonideal Plasmas @ Springer-Verlag Berlin Heidelberg (2005).
- [38] J. Lestessier and J. Rafelski, hadrons and quark-gluon plasma © Syndicate of the University of Cambridge (2002).
- [39] R. Abe, Progr. Theor. Phys. 21, 475 (1959).
- [40] F. Karsch and E. Laermann, hep-lat/0305025 v1, "quark-gluon plasma III" Rudolph C. Hwa (Editor), X. N. Wang (Editor) (2004).
- [41] G. Boyd, J. Engels, F. Karsch, E. Laermann, C. Legeland, M. Lütgemeier and B. Petersson, Phys. Rev. Lett. 75, 4169 (1995) and Nucl. Phys. B 469 419 (1996).
- [42] J. Engels, F. Karsh, H. Satz, and I. Montavay, Nucl. Phys. B205, 545 (1982).